Drosophila TAP/p32 is a core histone chaperone that cooperates with NAP-1, NLP, and nucleophosmin in sperm chromatin remodeling during fertilization

Alexander V. Emelyanov, Joshua Rabbani,[1] Monika Mehta, Elena Vershilova, Michael C. Keogh, and Dmitry V. Fyodorov

Department of Cell Biology, Albert Einstein College of Medicine, Bronx, New York 10461, USA

Nuclear DNA in the male gamete of sexually reproducing animals is organized as sperm chromatin compacted primarily by sperm-specific protamines. Fertilization leads to sperm chromatin remodeling, during which protamines are expelled and replaced by histones. Despite our increased understanding of the factors that mediate nucleosome assembly in the nascent male pronucleus, the machinery for protamine removal remains largely unknown. Here we identify four *Drosophila* protamine chaperones that mediate the dissociation of protamine–DNA complexes: NAP-1, NLP, and nucleophosmin are previously characterized histone chaperones, and TAP/p32 has no known function in chromatin metabolism. We show that TAP/p32 is required for the removal of *Drosophila* protamine B in vitro, whereas NAP-1, NLP, and Nph share roles in the removal of protamine A. Embryos from *P32*-null females show defective formation of the male pronucleus in vivo. TAP/p32, similar to NAP-1, NLP, and Nph, facilitates nucleosome assembly in vitro and is therefore a histone chaperone. Furthermore, mutants of *P32*, *Nlp*, and *Nph* exhibit synthetic-lethal genetic interactions. In summary, we identified factors mediating protamine removal from DNA and reconstituted in a defined system the process of sperm chromatin remodeling that exchanges protamines for histones to form the nucleosome-based chromatin characteristic of somatic cells.

[*Keywords*: sperm chromatin remodeling; protamines; fertilization; male pronucleus; histone chaperones; chromatin assembly]

Supplemental material is available for this article.

Received July 6, 2014; revised version accepted August 20, 2014.

The DNA of metazoan somatic cells is packaged into a compact nucleoprotein complex termed chromatin (Van Holde 1988; Wolffe 1998). Chromatin fiber is comprised of highly conserved repetitive units (nucleosomes) that contain an octamer of four core histones and 145–147 base pairs (bp) of DNA wrapped around the octamer in 1.65 turns of a left-handed superhelix (Luger et al. 1997). Nucleosomes are assembled in vivo in an ATP-dependent fashion through a concerted and sequential action of core histone chaperones and motor proteins that belong to the Snf2 family of DNA-dependent ATPases (Gorbalenya and Koonin 1993; Eisen et al. 1995; Mello and Almouzni 2001; Akey and Luger 2003; Haushalter and Kadonaga 2003; Piatti et al. 2011; Torigoe et al. 2013). For instance, *Drosophila* ACF/CHRAC can mediate chromatin assembly in conjunction with histone chaperone NAP-1 (Varga-Weisz et al. 1997; Ito et al. 1999). Other known ATP-dependent chromatin assembly factors include RSF, CHD1, ATRX, and ToRC/NoRC (LeRoy et al. 1998, 2000; Lusser et al. 2005; Lewis et al. 2010; Emelyanov et al. 2012).

The most abundant chromatin component in male germline cells is protamines—small positively charged arginine- and cysteine-rich proteins (Balhorn 2007). During spermiogenesis, protamines replace 85%–95% of DNA-bound histones in the nucleus to achieve a higher density of sperm nuclear DNA (Ward and Coffey 1991; Rathke et al. 2014). Crystalline-like sperm chromatin structure is sixfold more compact than metaphase chromosomes

[1]**Present address: Enzo Biochem, Incorporated, 527 Madison Avenue, New York, NY 10022, USA.**
Corresponding author: dmitry.fyodorov@einstein.yu.edu
Article is online at http://www.genesdev.org/cgi/doi/10.1101/gad.248583.114.

and renders sperm DNA enzymatically inert (Balhorn 1982). At fertilization, the oocyte remodels the condensed sperm chromatin into a transcriptionally competent chromatin of the male pronucleus (McLay and Clarke 2003). During, this process, protamines are expelled and replaced with oocyte-supplied histones, which are then organized into nucleosomes. Sperm chromatin remodeling (SCR) is controlled by biochemical activities in the early oocyte, but components of these activities remain largely unknown (McLay and Clarke 2003). However various protein factors have been implicated in SCR, including core histone chaperones from *Xenopus* (Nucleoplasmin, N1, HIRA, and TAF-I) and *Drosophila* (NAP-1, p22, DF31, HIRA, and Yemanuclein) (Dilworth et al. 1987; Philpott and Leno 1992; Kawasaki et al. 1994; Crevel and Cotterill 1995; Ito et al. 1996a; Matsumoto et al. 1999; Loppin et al. 2001; Ray-Gallet et al. 2002; Orsi et al. 2013). In mammals, members of nucleoplasmin/nucleophosmin family proteins (NPM1–3) function in sperm chromatin decondensation in vitro (Okuwaki et al. 2012). In addition, *Npm2* knockout female mice exhibit fertility defects consistent with a role of NPM2 in nuclear and nucleolar chromatin organization (Burns et al. 2003). It was also suggested that sperm chromatin decondensation is ATP-dependent (Wright and Longo 1988).

Drosophila melanogaster sperm cells contain two major protamines (A and B) encoded by male-specific transcripts *Mst35Ba* and *Mst35Bb*, respectively (Ashburner et al. 1999; Jayaramaiah Raja and Renkawitz-Pohl 2005). The *Drosophila* maternal effect mutant *sésame* (*ssm*) prevents male pronucleus formation (Loppin et al. 2001). *ssm* encodes the histone variant H3.3-specific chaperone HIRA (Tagami et al. 2004), postulated to be required for replication-independent deposition of histones in the male pronucleus during sperm decondensation (Loppin et al. 2005; Bonnefoy et al. 2007). In eggs from homozygous *ssm* females, maternal histones are not deposited in the chromatin of male pronuclei, preventing normal mitosis and resulting in the development of gynogenetic haploid embryos and embryonic stage lethality. A similar phenotype is observed in null mutants of the gene encoding ATP-dependent chromatin assembly factor CHD1 (Konev et al. 2007). Thus, CHD1 and HIRA act cooperatively and are required for nucleosome assembly during SCR. Intriguingly, protamines are efficiently expelled from the DNA of nascent male pronuclei in *Chd1* and *ssm* eggs (Jayaramaiah Raja and Renkawitz-Pohl 2005; Konev et al. 2007), suggesting that protamine removal and histone deposition are functionally distinct steps.

In this study, we used a biochemical approach to identify specific protein components of the *Drosophila* egg machinery that promote the dissociation of protamine–DNA complexes of sperm chromatin. These factors turn out to be two known core histone chaperones (NAP-1 and NLP), a homolog of mammalian nucleophosmin, and a novel *Drosophila* histone chaperone (TAP/p32). These putative "protamine chaperones" facilitate SCR independently of CHD1 and HIRA, which mediate nucleosome assembly in nascent male pronuclei. Of note, TAP/p32 is specifically required to expel *Drosophila* protamine B from sperm chromatin in vitro, whereas NAP-1, NLP, and nucleophosmin share roles in removal of protamine A. We also provide in vivo evidence that TAP/p32 functions in *Drosophila* egg SCR. In conclusion, we characterized protein factors that mediate the first obligatory step of SCR (protamine dissociation) and reconstituted the complete SCR reaction (reorganization of protamine-containing sperm chromatin into core histone-containing nucleosome arrays) in a purified defined system in vitro.

Results

Model sperm chromatin (MSC) substrate

To establish an in vitro assay for *Drosophila* SCR, we reconstituted a model substrate that contains the three major components of sperm chromatin: DNA and protamines A and B. To this end, we expressed and purified recombinant full-length polypeptides (untagged and C-terminally V5-tagged) encoded by *Mst35Ba* and *Mst35Bb* (*Drosophila* protamines A and B, respectively) (Supplemental Fig. S1A,B). Protamine–DNA complexes were reconstituted by dialyzing an equimolar mixture of protamines A and B (tagged or untagged) with a supercoiled 3.2-kb plasmid from high- to low-salt buffer (2 M to 0.2 M NaCl). Since the precise biochemical composition of native sperm chromatin is not known, we tested several molecular ratios of protein to DNA such that the resulting complexes would contain 1–2 bp of DNA for every positively charged amino acid (Arg, Lys, or His) of the proteins.

In our empirical optimization of the substrate, the major criteria for successful recapitulation of the properties of native sperm chromatin included (1) quantitative absorption of protamines by DNA and (2) the ability of the substrate to be processed in downstream biochemical manipulations in physiological conditions (see Fig. 1). Under these criteria, we decided to use a substrate that contains ~25 mol each of protamines A and B for every molecule of DNA (equivalent to ~64 bp of DNA for every protamine polypeptide or 1.6 bp of DNA for each basic residue in protamines). We term this reconstituted substrate model sperm chromatin (MSC).

To demonstrate that protamines form a stable complex with the DNA, we fractionated MSC by sucrose gradient sedimentation (Fig. 1A). Indeed, protamines cosedimented with plasmid DNA at the bottom of the gradient. The DNA template used for reconstitution encompassed five binding sites for yeast transcription factor GAL4 (Pazin et al. 1994). To examine the ability of the DNA-binding factor to interact with its recognition sequences, we performed in vitro chromatin immunoprecipitation (ChIP) (Lu et al. 2013) with naked plasmid DNA and MSC. Oligonucleosome arrays reconstituted by salt dialysis from plasmid DNA and *Drosophila* core histones were used as a control (Supplemental Fig. S1C). As expected, upon association with the DNA, protamines, similar to histones, strongly inhibited binding of recombinant GAL4-VP16. Thus, MSC exhibits a reduced ability to interact with DNA-binding factors.

We further analyzed MSC as a substrate in biochemical reactions with various nucleases (Supplemental Fig. S1D). Protamines interfered with efficient digestion of the DNA template by restriction endonuclease HaeIII and micrococcal nuclease. Unexpectedly, MSC exhibited increased sensitivity to DNase I relative to plasmid DNA. Therefore, protamines associated with DNA uniquely alter its biochemical properties in enzymatic reactions. In addition, we examined the ability of *Drosophila* topoisomerase I to relax negative DNA supercoils in the plasmid assembled into MSC (Supplemental Fig. S1E). We discovered that protamines associated with the DNA rendered it completely insensitive to topoisomerase I. We did not observe relaxation of the supercoiling at even the highest practical concentrations of the enzyme. Thus, MSC is not a substrate for topoisomerase I due to a very strong inhibition by associated protamines. Alternatively, not unlike core histones, protamines and DNA may establish topological domains that constrain negative DNA supercoiling.

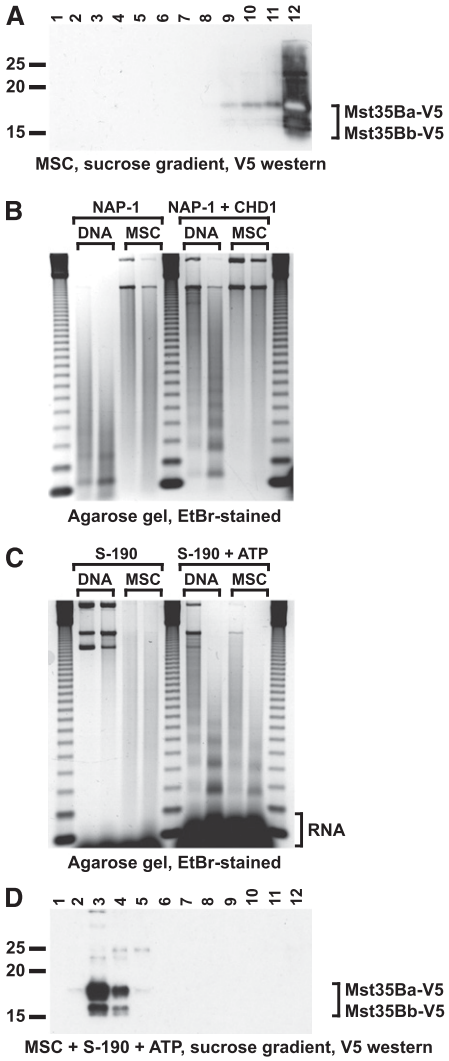

Nucleosome assembly and protamine eviction from MSC

The ATP-dependent chromatin assembly factor CHD1 and core histone chaperone HIRA are dispensable for the in vivo protamine removal from *Drosophila* sperm chromatin (Jayaramaiah Raja and Renkawitz-Pohl 2005; Konev et al. 2007). CHD1 supplemented with histone chaperones such as NAP-1 can assemble nucleosome arrays on protein-free DNA in vitro (Lusser et al. 2005). We decided to examine in vitro whether CHD1 and NAP-1 can assemble nucleosome arrays on MSC and replace protamines with core histones in vitro. Whereas plasmid DNA can be efficiently assembled into nucleosome arrays by CHD1 in the presence of NAP-1, MSC substrate could not be converted into nucleosomes (Fig. 1B). Thus, protamines are refractive to chromatin assembly in the purified recombinant ATP-dependent system. Crude *Drosophila* embryonic S-190 extract contains core histones and activities to assemble oligonucleosome arrays in an ATP-dependent manner (Fyodorov and Levenstein 2002). We hypothesized that S-190 may also contain activities to remove protamines from DNA, representing the native machinery of SCR. Indeed, S-190 extract can efficiently assemble oligonucleosome arrays on MSC substrate (Fig. 1C), and, similar to the assembly on naked DNA, this reaction requires ATP.

Next, we wanted to confirm that the resulting nucleosome-containing product is free of protamines. To this end, we subjected the product of chromatin assembly reaction with MSC and S-190 to sucrose gradient sedimentation (Fig. 1D) and determined that protamines were no longer associated with the DNA and sedimented in

Figure 1. SCR activity of *Drosophila* embryonic extract. (*A*) Sucrose gradient sedimentation of MSC substrate. MSC was fractionated on sucrose gradient, and gradient fractions were analyzed for the presence of V5-tagged protamines by Western blotting. Protamines cosediment with DNA at the bottom of the gradient (fraction 12). Molecular masses (in kilodaltons) and positions of protein marker bands are shown at the *left*, and fraction numbers are shown at the *top*. The bracket at the *right* designates the expected positions of protamines A and B on the Western blot. (*B*) Protamines inhibit oligonucleosome assembly in a purified recombinant system. Nucleosome arrays were assembled by an ATP-dependent system with native core histones and recombinant NAP-1 and CHD1 on naked DNA and MSC templates. Chromatin assembly was assayed by partial micrococcal nuclease digestion and agarose gel electrophoresis. DNA was stained with ethidium. Lanes at the *left* side, in the middle, and at the *right* side show the 123-bp DNA ladder. (*C*) S-190 extract can assemble nucleosome arrays on MSC substrate. Chromatin assembly was performed and assayed as in *B* with the S-190 extract from *Drosophila* embryos. The bracket at the *left* designates the position of contaminating RNA from the S-190 extract. (*D*) Sucrose gradient sedimentation of S-190-remodeled MSC substrate. Products of the S-190-mediated chromatin assembly reaction on MSC substrate (shown in *C*) was fractionated and analyzed as in *A*. Protamines are physically removed from DNA by treatment with the S-190 extract.

earlier fractions. Thus, S-190 extract contains biochemical activities that physically dissociate a protamine–DNA complex under physiological conditions. ATP only slightly modulates protamine eviction by the S-190 extract: When MSC was treated with the extract without ATP and subjected to sucrose gradient sedimentation, the vast majority of protamines sedimented in lighter, DNA-free fractions (Fig. 2A). Thus, S-190 dissociates protamines from MSC in an ATP-independent manner. In control reactions with substrates that contained higher concentrations of protamines (1–1.3 bp of DNA per basic residue of protamine molecules), S-190 extract performed poorly in protamine eviction, which suggested that substrates with excessive protamine content do not represent a proper physiological model of sperm chromatin (data not shown).

Putative protamine chaperones of Drosophila *S-190 extract*

We hypothesized that S-190 extract contains molecular chaperone proteins that physically interact with protamines and compete for their binding with DNA. If true, these proteins are likely to remain associated with protamines after their eviction from DNA, so we attempted to isolate them by pull-down of V5-tagged protamines from DNA-free fractions of the sucrose gradient (Fig. 2A). Protamine-containing complexes were purified by V5 immunoaffinity chromatography and analyzed by SDS-PAGE (Fig. 2B). For control pull-downs, V5 antibody-interacting proteins were isolated from the extract in the absence of MSC. We identified five major polypeptides with apparent molecular masses of 110, 48, 25, 24, and 22 kDa that specifically associate with protamines upon their removal from MSC. Mass spectrometry analyses of the bands identified them as *Drosophila* proteins NAP-1, CG6459, CG7911, and NLP (Supplemental Table S1). The 110-kDa band could not be reliably assigned to a known *Drosophila* protein: Of 137 peptide matches, only six corresponded to a predicted protein, CG31731. The polypeptides in purified material are present in varying concentrations, which may result from their distinct relative affinities toward protamines. However, most likely, this difference reflects their variable abundance in the extract. For instance, NAP-1, which is highly represented in the protamine chaperone material, is known to be very abundant in the embryo and S-190 extract. Thus, it is possible that we may not have discovered additional, less abundant, putative protamine chaperones.

We next examined whether the putative protamine chaperones bind differentially to protamines A and B. To this end, we reconstituted MSC substrates with only one of the molecules V5-tagged. For instance, if MSC is reconstituted with untagged protamine A and tagged protamine B and subjected to remodeling with S-190, only protamine B-bound molecules will be purified by V5

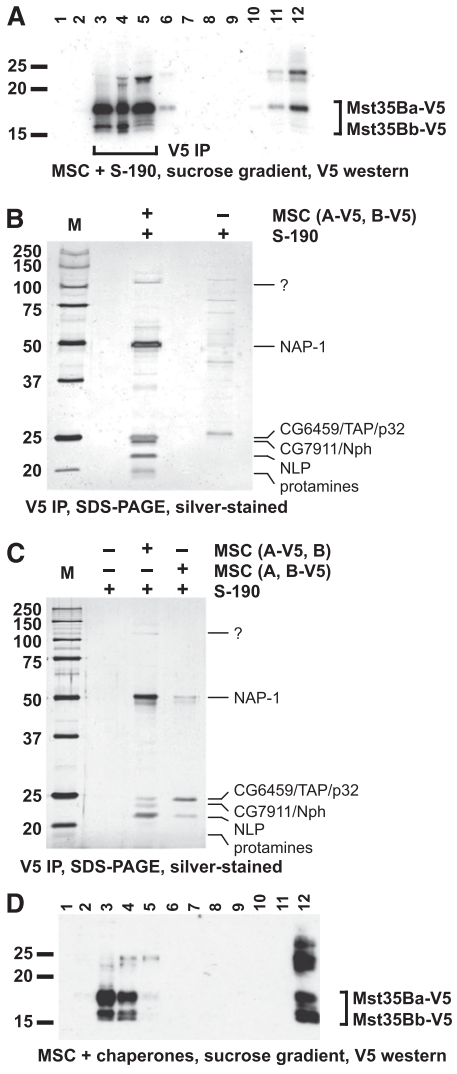

Figure 2. Putative protamine chaperones. (*A*) MSC remodeling by S-190 does not require ATP. S-190-mediated protamine eviction from MSC was examined as in Figure 1D in the absence of ATP and ATP regeneration system. The bracket at the *bottom* designates fractions (3–5) used for V5 immunoprecipitation of protamines and associated proteins. (*B*) Putative protamine chaperones copurify with protamines post-MSC remodeling. SDS-PAGE of proteins coimmunoprecipitating with protamines removed from MSC. (*Right* lane) Proteins immunoprecipitated by V5 antibody from unfractionated S-190 extract in the absence of V5-tagged protamines or MSC. (*Left* lane) Protein molecular mass marker. Molecular masses of marker proteins are shown at the *left* (in kilodaltons), and identities and positions of protein bands as determined by mass spectrometry sequencing are shown at the *right*. (*C*) Putative protamine chaperones exhibit specificity toward protamine A or B. Protamine-associated complexes were isolated as in *B* from remodeling reactions that contained MSC substrates reconstituted with one V5-tagged and one untagged protamine polypeptide. TAP/p32 exhibits a stronger preference for protamine B, whereas NAP-1, NLP, and Nph exhibit a stronger preference for protamine A. Control lanes contain material immunoprecipitated by V5 antibody from fractions 3–5 of S-190 extract subjected to sucrose gradient as in *A*. (*D*) MSC remodeling by recombinant protamine chaperones. MSC was remodeled by an equimolar mixture of recombinant putative protamine chaperones and analyzed as in *A*.

chromatography. In this manner, we were able to specifically isolate protamine A- and protamine B-containing complexes (Fig. 2C). We discovered a substantial bias in the binding properties of their putative protamine chaperones. Whereas NAP-1, CG7911 and NLP were highly represented in protamine A-bound complexes, they associated much more weakly with protamine B. On the contrary, CG6459 was highly represented in complexes with protamine B, where it efficiently outcompeted the apparently more abundant NAP-1. Therefore, native protamine chaperones exhibit partial specificity toward particular protamines.

Although the putative chaperones bind protamines after their removal from MSC, it is possible that these complexes form only after protamines have already been dissociated from DNA by a different set of factors in the S-190 extract. To investigate this possibility, we reconstituted these proteins in a recombinant form (Supplemental Fig. S2A) and assayed for a potential SCR activity. When a mixture of all four putative chaperones was incubated with MSC (~5 mol of each chaperone for every protamine molecule present in MSC), protamines could be efficiently released from the substrate (Fig. 2D). Thus, protamine chaperones NAP-1, CG6459, CG7911, and NLP are sufficient for dissociation of protamines from DNA.

NAP-1, NLP, Nph (CG7911), and TAP/p32 (CG6459)

Drosophila NAP-1 and NLP are known core histone chaperones that can mediate histone deposition and removal from DNA (Ito et al. 1996a,b). dNAP-1 (but not NLP) has also been shown to function in decondensation of *Xenopus* sperm chromatin in vitro (Ito et al. 1996a). However, *Xenopus* sperm decondensation uses a heterologous substrate and does not provide direct evidence for the ability of assayed proteins to remodel sperm chromatin. In contrast, our results directly demonstrate that *Drosophila* NAP-1 and NLP can function in the removal of protamines from *Drosophila* sperm chromatin, although the activity is weak.

The predicted protein CG7911 is highly homologous to NLP, with BLAST alignment indicating that *CG7911* encodes an ortholog of mammalian NPM1–3, which belong to the nucleoplasmin superfamily of histone chaperones. Therefore, we term the CG7911 protein as *Drosophila* nucleophosmin and the cognate gene *Nph*. CG7911/Nph may be related to the basic heat-stable protein p22, isolated from *Drosophila* extract, based on *Xenopus* sperm decondensation assay (Kawasaki et al. 1994).

CG6459 does not share sequence similarity with NAP-1, NLP, or Nph. It is a fly ortholog of mammalian protein p32/HABP1/gC1q-R/TAP. TAP/p32 was originally isolated as a protein that binds and inhibits an essential cellular splicing factor, ASF/SF2 (Krainer et al. 1990; Petersen-Mahrt et al. 1999). TAP/p32 also inhibits splicing of HIV transcripts (Berro et al. 2006); its interaction with the HIV Rev protein promotes export of unspliced HIV RNA (Tange et al. 1996). TAP/p32 physically interacts with plasma complement component C1q and inhibits its hemolytic activity (Ghebrehiwet et al. 1994). Finally, TAP/p32 was proposed to function in transcriptional regulation: Human TAP/p32 contains a functional transcriptional activation domain in its C terminus (Yu et al. 1995) and interacts with multiple viral (HIV transactivator Tat, EBNA-1 of Epstein-Barr virus, ORF P of HSV, and core protein V of adenovirus) and cellular (TFIIB, lamin B receptor, and vitronectin) proteins (Bruni and Roizman 1996; Wang et al. 1997; Matthews and Russell 1998). *Drosophila* CG6459 is also homologous to budding yeast (*Saccharomyces cerevisiae*) Mam33 (*YIL070C*), a mitochondrial matrix protein involved in the maintenance of oxidative phosphorylation (Muta et al. 1997). *Drosophila CG6459* (*P32*) was recently shown to regulate neurotransmitter release in vivo at adult neuromuscular synapses by an unknown mechanism (Lutas et al. 2012). However, its role in chromatin metabolism has not yet been reported, and its true physiological functions in metazoans remain obscure.

Although *Drosophila* TAP/p32 shares no sequence similarity with the other protamine chaperones (NAP-1, NLP, or Nph), human TAP/p32 is structurally related to *Xenopus* nucleoplasmin (Dutta et al. 2001) and *Drosophila* NLP (Namboodiri et al. 2003). X-ray crystallography of human TAP/p32 (Jiang et al. 1999) reveals a donut-shaped homotrimeric complex with the shape and size (~75 Å outer diameter, ~20 Å inner diameter, and ~30 Å thickness) similar to those of pentameric NLP (~60 Å outer diameter, ~10 Å inner diameter, and ~50 Å thickness). Moreover, both TAP/p32 and nucleoplasmin/NLP exhibit similar uneven charge distribution, with basic amino acids presented on one side of the "donut" and in the inner "hole."

Protein interaction networks for many *Drosophila* proteins have recently been studied by coaffinity purification and mass spectrometry (Guruharsha et al. 2011). Interestingly, TAP/p32, NLP, and Nph share a large number of partners in their interaction maps (Supplemental Fig. S2B), with >59% of possible Nph-binding proteins also associating with NLP or TAP/p32 (or both). In comparison, there is no substantial overlap between the protamine chaperone interaction networks and that of Hsp60, a mitochondrial marker (Supplemental Fig. S2B).

To further substantiate a relationship among the putative protamine chaperones, we compared their subcellular distribution in *Drosophila* embryos. We fractionated nuclei and mitochondria by a series of centrifugation steps (Kang et al. 1995) and examined the localization of NAP-1, NLP, Nph, and TAP/p32 by immunoblotting (Supplemental Fig. S2C). NLP and Nph were present in nuclear and cytosolic fractions but completely absent from mitochondria; NAP-1 was found in all three fractions, while TAP/p32 was localized to nuclei and mitochondria but almost completely excluded from the cytosol. The mitochondrial enrichment of TAP/p32 may suggest a role comparable with that of its *S. cerevisiae* homolog, Mam33. However the observation that all four putative protamine chaperones are highly abundant in nuclei is consistent with the roles that they may play in chromatin metabolism.

Genetic analyses of S. cerevisiae *Mam33*

Drosophila TAP/p32 is homologous to *S. cerevisiae* Mam33, a poorly characterized protein localized to the mitochondrial matrix (Muta et al. 1997; Reinders et al. 2006). To examine potential roles for Mam33p in vivo, we prepared a deletion allele (*mam33Δ*) and compared its loss of function with a strain deleted for the mitochondrial morphology regulator She9 (Mdm33p, *YDR393W*) (Messerschmitt et al. 2003; Hoppins et al. 2011). Both strains (*mam33Δ* and *she9Δ*) fail to grow on nonfermentable carbon sources (Supplemental Fig. S3A), supporting their roles in the function of mitochondria. Unexpectedly, we discovered that *mam33Δ* but not *she9Δ* exhibited elevated sensitivity to the DNA-alkylating genotoxin MMS (Supplemental Fig. S3B). This observation suggests extramitochondrial roles for Mam33p, including chromatin function and DNA damage response.

Genome-scale genetic interaction screening is a powerful tool to investigate the relationship between factors, where a negative (synthetic-sick/synthetic-lethal [SS/SL]) interaction between two alleles often indicates that their gene products impinge on the same essential function (Beltrao et al. 2010). To understand the biological roles of Mam33 in a greater detail, we analyzed its genetic interactions with a collection of ~4800 nonessential yeast gene deletions (covering ~80% of all genes) by a synthetic genetic array (SGA) screen. As might be expected, the *mam33Δ* allele exhibits negative genetic interactions with a range of mitochondrial regulator genes, such as the α-ketoglutarate dehydrogenase subunit *KGD1*, and inner membrane proteins *SHE9* and *MDM31* (Supplemental Table S2). However, additional genetic interactions are suggestive of roles for Mam33 in DNA recombination/repair (*RAD52*, *MMS22*, *BRE1*, and *MPH1*), chromatin remodeling (subunits of SWI/SNF family complexes Ino80, Isw1b, SWR, RSC, and SWI/SNF), and DNA compaction (*SPE1*, *SPE2*, and *SPE3*, essential for synthesis of positively charged polyamines) (Supplemental Fig. S3C; Balasundaram et al. 1994; Hamasaki-Katagiri et al. 1997). Thus, the yeast ortholog of TAP/p32 plays biological roles in nuclear DNA/chromatin metabolism.

MSC remodeling by protamine chaperones

To further understand specific functions of the newly identified protamine chaperones in SCR, we studied their activities (individually and in various combinations) in protamine release from MSC. To facilitate these analyses, we adopted a streamlined SCR assay in which protamine association with DNA (Fig. 3A) and release from the MSC substrate (Fig. 3B) were monitored by size exclusion chromatography. DNA-containing MSC fractionated in the void volume, whereas protamines evicted from MSC eluted in later fractions of gel filtration columns. Thus, for reaction product analyses, only the void volume (DNA-"bound" protamines) and pooled fractions 2 and 3 (DNA-"free" protamines) need to be examined by immunoblotting.

The kinetics of SCR exhibits dose dependence on the concentration of protamine chaperones (Fig. 3C). Also, as expected for a decomposition biochemical reaction in solution, protamines were released by chaperones in a time-dependent manner (Fig. 3D). When MSC substrates that contain only one tagged protamine were treated with recombinant protamine chaperone proteins individually, we observed extremely inefficient dissociation of the DNA–protamine complexes (Fig. 3E). Different chaperones could evict protamine A with a variable degree of efficiency, with TAP/p32 exhibiting the strongest eviction activity among all chaperones. Importantly, only TAP/p32 was able to release protamine B. This result is consistent with a higher specificity of native TAP/p32 to protamine B in MSC remodeling by the S-190 extract (Fig. 2C) and further supports a model of unique contributions by the collection of protamine chaperones to SCR. A strong synergy between different chaperones was demonstrated in another experiment (Fig. 3F). Although the activity of an equimolar mixture of all four chaperones in MSC remodeling compares with that of the S-190 extract, neither the mixture of NAP-1, NLP, and Nph nor TAP/p32 alone (at four times the normal concentration) could efficiently remove protamines from DNA. It appeared that both protamines A and B had to be released simultaneously to achieve strong eviction. Significantly, supplementing TAP/p32 with only one of the other three chaperones was sufficient to stimulate MSC remodeling reactions (Supplemental Fig. S2D). Thus, NAP-1, NLP, and Nph share functions in SCR in vitro and additionally require TAP/p32 for optimal activity in the release of protamines.

The analyses of the time course of the reaction with various combinations of chaperones (Fig. 3G) further emphasized the requirement for synergistic action of TAP/p32 and the other protamine chaperones. Although close to 100% of protamines are evicted from MSC after prolonged incubation with a mixture of NAP-1 and TAP/p32, neither TAP/p32 nor a mixture of NAP-1, NLP, and Nph can bring about quantitative removal of protamines A and B. In summary, our analyses of biochemical activities of *Drosophila* NAP-1, NLP, Nph, and TAP/p32 suggest a model of individualized functions for TAP/p32 and the other protamine chaperones. Specifically, TAP/p32 is essential for removal of protamine B from sperm chromatin, whereas NAP-1, NLP, and Nph play roles in removal of protamine A. A combination of these two activities is required for efficient disassembly of sperm chromatin that contains both protamines A and B.

Biological function of Drosophila *TAP/p32*

Because it appears that TAP/p32 plays a key, nonredundant role in SCR in vitro, we decided to analyze its function in *Drosophila* in vivo. To this end, we prepared null mutant alleles of *P32* by homologous recombination-based gene targeting (Supplemental Fig. S4A,B). In addition, we generated a double-null mutant allele of *Nlp* and *Nph* by imprecise *P*-element excision (Supplemental Fig. S4C,D).

P32 mutation, unlike the mutation of *Nlp* and *Nph*, resulted in a significant decrease of viability of adult homozygous progeny in crosses of heterozygous mutant parents (Table 1). The fecundity of homozygous *P32* females

was also strongly reduced. Null females (2–5 d old) mated to *P32*-null or wild-type males deposited a reduced number of eggs (about seven per mother per day compared with ~55 for wild-type females). Despite an apparently normal morphology, <5% of deposited homozygous-null mutant embryos hatched into L1 larvae, compared with 104% for the wild type under optimal conditions (25°C, 60% air humidity). (A >100% calculated survival rate for wild-type embryos indicates that some of the laid eggs were not detected.) Although adult escapers could be observed in inter se crosses of homozygous mutant parents, both female fecundity and viability/development of the progeny were compromised. Thus, *P32* is important for oogenesis and is maternal-effect essential for embryonic viability or fertilization.

In addition, *P32* females exhibited a prolonged egg retention phenotype similar to that of *dunce* mutants (Bellen et al. 1987) and females ablated of spermathecal secretory cells (SSCs) prior to mating (Schnakenberg et al. 2011). *P32*-null mutation results in facultative ovoviviparity: Deposition of embryos by *P32* females was delayed, with the majority of embryos deposited after extended development inside their mothers' ovaries. When we examined developmental stages of *P32/P32* embryos by propidium iodide (PI) staining 2 h after egg deposition (AED) (Supplemental Table S3), we detected up to 19% of embryos in advanced, post-nuclear blastoderm stages, compared with only ~3% of wild-type embryos. This number was only moderately increased after an additional 2 h of development (from ~19% to ~33% for *P32* mutant embryos), in contrast to wild-type embryos, where the relative number of advanced stage animals increased from ~3% to ~29%.

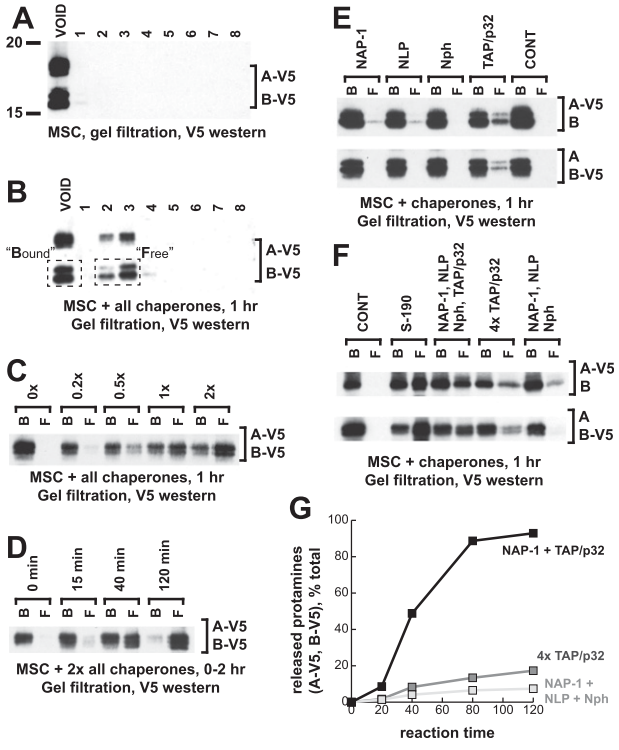

Interestingly, a large fraction of *P32* embryos from 0 to 4 h AED remained in very early stages of development (~34%, compared with ~11% for the wild type). This phenotype closely resembles one that we reported previously for *Chd1* mutant embryos (Konev et al. 2007), which exhibit deficient nucleosome assembly in the male pronucleus. Closer inspection of syncytial *P32* mutant embryos in the anaphase stage of the cell cycle revealed a reduced amount of chromosomal DNA in ~74% of them (Fig. 4A), consistent with a haploid DNA content. Thus, similar to *Chd1* and *ssm* mutants (Loppin et al. 2005; Konev et al. 2007), *P32*-null females may have chromatin assembly and/or SCR compromised.

Because *P32* alleles are extremely weak, we were unable to generate fertile alleles in which a mutation of *P32* is combined with a transgene expressing tagged Mst35Ba

Figure 3. Biochemical activities of protamine chaperones in MSC remodeling. (*A*) Size exclusion chromatography of MSC substrate. MSC was fractionated by gel filtration, and column fractions were analyzed for the presence of V5-tagged protamines by Western blotting. Protamines copurify with DNA in the void volume (VOID). Molecular masses (in kilodaltons) and positions of protein marker bands are shown at the *left*, and fraction numbers are shown at the *top*. The bracket at the *right* designates the expected positions of protamines A and B on the Western blot. (*B*) Size exclusion chromatography of MSC remodeled by recombinant protamine chaperones. MSC was remodeled by an equimolar mixture of recombinant protamine chaperones (2.3 μM each) and analyzed as in *A*. Void volume (VOID) contained residual DNA-bound protamines, whereas fractions 2 and 3 contained protamine molecules evicted from MSC (dashed frames). (*C*) Protamine chaperone dose dependence of MSC remodeling reaction. MSC substrate containing all V5-tagged versions of protamines A and B was remodeled with increasing amounts of an equimolar mixture of recombinant protamine chaperones (from 0.46 to 4.6 μM each). After gel filtration, void volume and fractions 2 and 3 were analyzed by V5 Western for the presence of DNA-bound (B) or DNA-"free" (F) protamines, respectively. (*D*) Time course of MSC remodeling by a mixture of protamine chaperone. MSC substrate containing all V5-tagged versions of protamines A and B was remodeled with an equimolar mixture of recombinant protamine chaperones (4.6 μM each) for various times and analyzed as in *C*. (*E*) Inefficient protamine eviction by individual chaperones. MSC substrates were reconstituted with one V5-tagged and one untagged protamine polypeptide. Remodeling reactions were performed in the presence of individual protamine chaperone polypeptides (2.3 μM) as indicated at the *top* or in the absence thereof (CONT). MSC remodeling was analyzed as in *C*. (*F*) Synergism and partial specificity of protamine chaperones in MSC remodeling. MSC substrates were prepared; remodeled with various combinations of protamine chaperones (2.3 μM each), TAP/p32 alone (9.2 μM), or S-190 extract; and analyzed as in *C*. (*G*) Time course of MSC remodeling by protamine chaperones. MSC substrate containing all V5-tagged versions of protamines A and B was remodeled with 2.3 μM each NAP-1 and TAP/p32 (black line); 2.3 μM each NAP-1, NLP, and Nph (light-gray line); or 9.2 μM TAP/p32 (dark-gray line) for various times (0–120 min) and analyzed as in *C*. Western blots were exposed to X-ray film, and chemilluminescence signals for individual bands were quantitated by film densitometry and plotted.

Table 1. *Viability of* Nlp/Nph *and* P32 *mutants*

Cross	Progeny scored	Viability	Percentage expected
Nph^{Nlp}/CyO X $P32^{5}/CyO$[a]	$Nph^{Nlp}/P32^{5}$	35/86 (29)	121%
$P32^{2}/CyO$ X $P32^{4}/CyO$	$P32^{2}/P32^{4}$	14/110 (37)	**38%, $P < 10^{-5}$**
$P32^{2}/CyO$ X $Df(2R)Exel7149/CyO$	$P32^{2}/Df(2R)Exel7149$	19/187 (62)	**31%, $P < 10^{-8}$**
$Nph^{Nlp}/TM6B$ X $Nph^{Nlp}/TM6B$	Nph^{Nlp}/Nph^{Nlp}	52/88 (44)	118%
$Nph^{Nlp}/TM6B$ X $Df(3R)Exel6213/TM6B$	$Nph^{Nlp}/Df(3R)Exel6213$	24/56 (19)	126%

Parents that carry heterozygous mutant alleles of *Nlp/Nph* and *P32* were crossed inter se or as shown in the first column, and adult progeny of various genotypes (second column) were scored based on phenotypic manifestations of balancer markers (*Cy* in *CyO* and *Hu* in *TM6B*, *Tb*). Viability numbers (third column) are presented as numbers of the scored progeny relative to the total progeny numbers; expected numbers based on the Mendelian genetic distribution are shown in parentheses. The percentage expected viability (fourth column) is calculated by dividing the number of progeny of the indicated genotype by the expected number. Results representing highly statistically significant effect on viability are shown in bold. Probability values are calculated by the χ^2 two-way test.
[a]Wild-type control cross. *Df(2R)Exel7149* and *Df(3R)Exel6213* uncover *P32* and *Nlp/Nph* loci, respectively.

or Mst35Bb. Thus, we could not directly observe a defect in protamine removal by homozygous *P32* eggs. However, in *P32* embryos that remained in early stages of development (>33%), we frequently observed apposed male and female pronuclei, of which only one was undergoing mitosis, whereas the other remained condensed and did not divide in synchrony (Fig. 4B). This phenotype is strongly reminiscent of that in *Chd1* mutants, which are unable to form functional male pronuclei due to disrupted assembly of H3.3-containing chromatin on paternal DNA after protamine removal (Konev et al. 2007). Considering that MSC is refractive to nucleosome assembly by CHD1 in vitro without prior removal of protamines (Fig. 1B), it is very likely that *P32* mutation affects protamine removal during fertilization, which in turn prevents further biochemical processing of paternal chromosomes by CHD1 and HIRA.

In addition to the apparent phenotype in SCR, early *P32* mutant embryos exhibited a spectrum of other chromosomal abnormalities, including anaphase bridges and chromosome breaks (Fig. 4C). These phenotypes are also suggestive of a biological function for TAP/p32 in chromosome structure/stability during syncytial division cycles. Importantly, fertility was not affected, and none of the described microscopic phenotypes were noticed in homozygous double *Nlp/Nph* mutants, which is consistent with partially redundant biochemical functions of NAP-1, NLP, and Nph. Together with our in vitro results, the in vivo analyses suggest that TAP/p32 plays an essential unique role in sperm chromatin metabolism, such as eviction of protamine B. Although it has to be supplemented with NAP-1, NLP, or Nph to achieve efficient unraveling of sperm chromatin, the latter may share partially redundant functions with each other, such as eviction of protamine A.

Histone chaperone activity of TAP/p32

The *Nap1*-null mutant allele is homozygous-lethal (Stephens et al. 2006), whereas *Nlp/Nph* and *P32* are not. To better understand interactions among protamine chaperones in vivo, we combined *Nlp/Nph* and *P32* mutations and discovered significant recessive and dominant interactions (Table 2). Heterozygous *P32* mutation reduced the viability of homozygous *Nlp/Nph* mutants, and *Nlp/Nph* was a recessive enhancer of *P32* lethality. These results provide further strong indications of common biological functions for these protamine chaperones. Importantly, these functions appear to be shared not exclusively in the embryo but during later stages of development because genetic interactions were observed in crosses of heterozygous parents that carry maternally deposited factors, and partial lethality occurred in late larvae. Since NLP is a known histone chaperone and functions in nucleosome assembly and disassembly, we hypothesized that Nph and TAP/p32 are also core histone chaperones.

We analyzed potential physical interaction of these proteins with core histones by glycerol gradient sedimentation (Fig. 5A). We discovered that, similar to NAP-1 and NLP, Nph and TAP/p32 physically associate with *Drosophila* core histones. Furthermore, TAP/p32 exhibits a higher apparent affinity toward histones H3 and H4, whereas H2A and H2B associate with TAP/p32 only weakly. Whereas physical interactions could be predicted for Nph based on its sequence conservation with NLP and mammalian nucleophosmins, histone binding of TAP/p32 is a novel, unpredicted biochemical function for this protein. Core histone chaperones can cooperate with ATP-dependent factors, such as ACF, in the assembly of nucleosome arrays from DNA and core histones in vitro (Ito et al. 1997). We decided to assay TAP/p32 in the purified nucleosome assembly system for its ability to facilitate histone deposition. We found that TAP/p32 can assemble chromatin in conjunction with ACF (Fig. 5B). This result corroborates our analyses of histone-TAP/p32 physical interactions and confirms that TAP/p32 functions as a core histone chaperone.

The latter result provided us with an opportunity to recapitulate in vitro the complete process of SCR during fertilization, which involves protamine removal from paternal sperm chromatin with subsequent deposition of maternally provided core histones and formation of regular nucleosome arrays characteristic of somatic cell chromatin. In our exploration of a minimal set of protein factors that is sufficient for SCR reaction, we discovered that supplementing the standard ATP-dependent nucleosome assembly system (NAP-1 and ACF) with TAP/p32 makes it competent in nucleosome assembly on the MSC

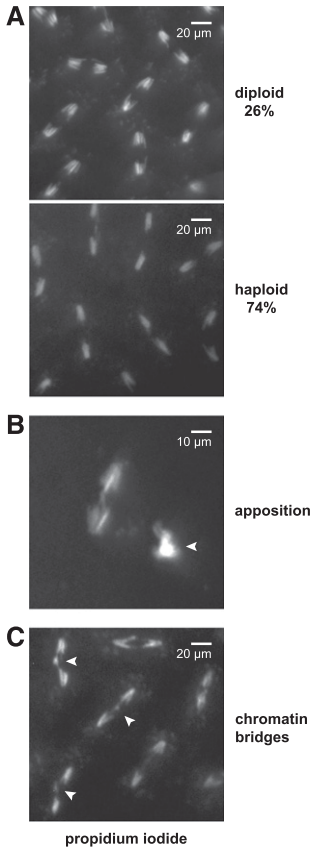

Figure 4. Mitotic defects of *P32*-null embryos. (*A*) High proportion of haploid syncytial embryos in the progeny of *P32*-null parents. PI-stained syncytial embryos were observed in mitosis, and anaphase embryos were scored as diploid (*top* panel) or haploid (*bottom* panel) based on their appearance. Division cycles 9 and 10 are shown. Numbers at the *right* indicate distribution in a sample of 250 anaphase embryos. Bars, 20 μm. (*B*) Mitotic failure of a nascent pronucleus during apposition in *P32*-null embryos. The absence of maternal TAP/p32 frequently results in the inability of one pronucleus (arrowhead) to enter the first mitosis. Bar, 10 μm. (*C*) Chromatin (anaphase) bridges and chromosome breaks in *P32*-null embryos. *P32* embryos exhibit incomplete segregation of sister chromatids. More than 50% of syncytial embryos in anaphase exhibit one or more chromatin bridges (arrowheads). Bar, 20 μm.

substrate (Fig. 5C). Thus, we were able to recapitulate in a purified system in vitro chromatin transitions that paternal DNA undergoes during fertilization. We conclude that *Drosophila* core histone chaperones NAP-1 and TAP/p32 (along with HIRA, NLP, and Nph) and ATP remodeling factors such as CHD1 and ACF represent core biochemical machinery required for SCR in vitro and in vivo.

Discussion

Although recent studies provide details of sperm chromatin composition (Hammoud et al. 2009; Miller et al. 2010) and assembly during spermiogenesis (Rathke et al. 2014), relatively little is known about the protein machinery that mediates SCR during fertilization (Orsi et al. 2013). In vivo analyses in *Drosophila* suggest that removal of protamines from sperm chromatin is biochemically uncoupled from subsequent nucleosome assembly (Jayaramaiah Raja and Renkawitz-Pohl 2005; Konev et al. 2007) because male pronucleus-specific nucleosome assembly factors CHD1 and HIRA are not required for protamine removal. Our study demonstrates that, indeed, a separate set of protein factors (protamine chaperones) is required for protamine eviction (Fig. 1). Using assay-based biochemical approaches, we identified four *Drosophila* proteins that are sufficient for unraveling of DNA–protamine complexes in vitro (Fig. 2). We analyzed their biochemical activities and mechanisms of SCR (Fig. 3). Significantly, we were able to recapitulate the entire process of SCR (protamine eviction and nucleosome assembly) in a defined purified system (Fig. 5C). We further examined biological functions of TAP/p32 in *Drosophila* and obtained evidence of its proposed roles in SCR in vivo (Fig. 4). Finally, we discovered that all four proteins additionally share a function as core histone chaperones (Fig. 5).

Recent microarray analysis of mating-responsive genes in *Drosophila* (Mack et al. 2006) revealed that *CG6459/P32* expression is strongly activated in the female lower reproductive tract within 6 h of mating. In fact, *CG6459/P32* exhibits the strongest response of all genes identified in the study. The up-regulation is transient: It is reversed 24 h after mating. This temporal expression pattern of TAP/p32 further supports its proposed role during fertilization.

Intriguingly, orthologs of protamine chaperones are expressed in unicellular organisms, such as *S. cerevisiae*, which do not express protamines and whose gametes do not undergo the chromatin reorganization characteristic of metazoan sperm cells. We provide evidence that Mam33p, an *S. cerevisiae* ortholog of TAP/p32, is involved in chromatin remodeling and DNA compaction and/or repair (Supplemental Fig. S3). It is likely that protamine chaperone homologs in unicellular eukaryotes perform conserved functions of core histone chaperones

Table 2. *Interactions among protamine chaperone genes*

Cross	Progeny scored	Viability	Percentage expected
$P32^{2}$/CyO; Nph^{Nlp}/TM6B $_{X}$ $P32^{4}$/CyO; Nph^{Nlp}/TM6B	P32/CyO; Nph^{Nlp}/Nph^{Nlp}	28/98 (33)	**85%, $P < 10^{-4}$**
P32/CyO; Nph^{Nlp}/Nph^{Nlp} $_{X}$ P32/CyO; Nph^{Nlp}/Nph^{Nlp}	P32/P32; Nph^{Nlp}/Nph^{Nlp}	10/172 (57)	18%, $P < 0.05$

Parents that carry combinations of heterozygous or homozygous mutant alleles of *Nlp/Nph* and *P32* were crossed inter se or as shown in the first column, and adult progeny of various genotypes (second column) were scored based on phenotypic manifestations of balancer markers (*Cy* in *CyO* and *Hu* in *TM6B*, *Tb*). Viability numbers and probability values were calculated and are presented as in Table 1.

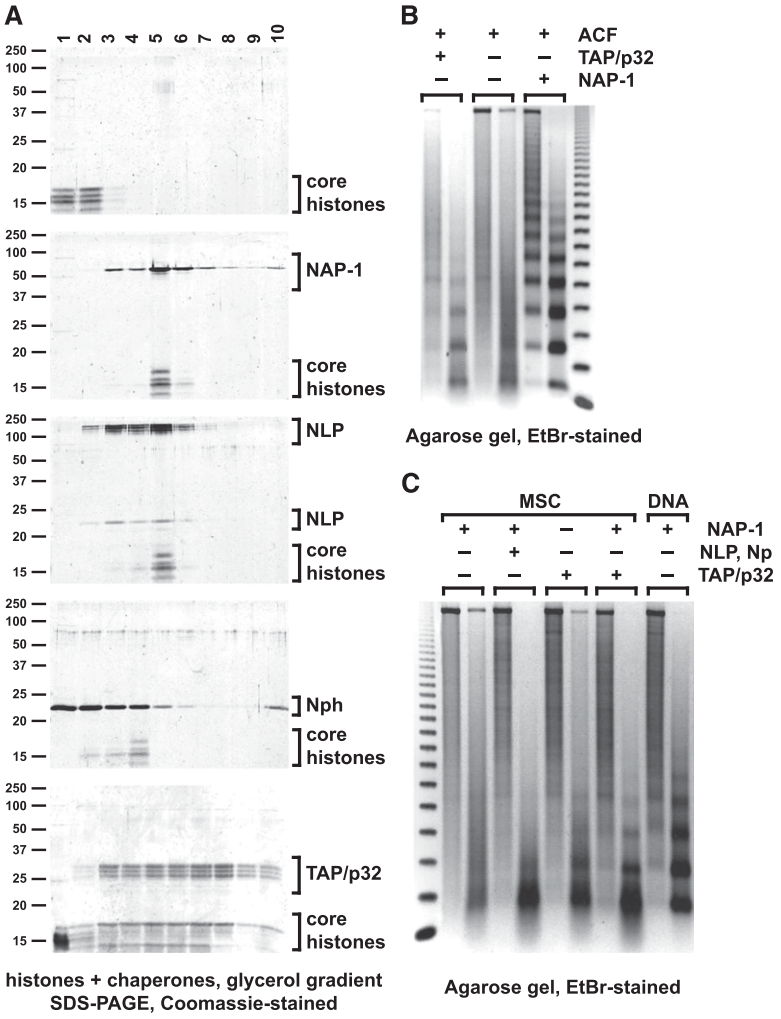

Figure 5. Core histone chaperone activity of protamine chaperones. (*A*) Physical interactions of core histones with recombinant NAP-1, NLP, Nph, and TAP/p32. Protein–core histone mixtures were subjected to glycerol gradient sedimentation, and gradient fractions were analyzed by SDS-PAGE and staining with Coomassie. (From *top* to *bottom*) Histones only, histones + NAP-1, histones + NLP, histones + Nph, and histones + TAP/p32. Molecular masses (in kilodaltons) and positions of protein marker bands are shown at the *left*. (*B*) TAP/p32 can substitute for NAP-1 in an ATP-dependent purified recombinant nucleosome assembly system. Nucleosome arrays were assembled on naked DNA by the ATP-dependent system with native core histones and recombinant ACF in the absence or presence of chaperones TAP/p32 or NAP-1. Chromatin assembly was assayed by partial micrococcal nuclease digestion and agarose gel electrophoresis. DNA was stained with ethidium. (*Right* lane) The 123-bp DNA ladder. (*C*) Recapitulation of SCR process in vitro. Nucleosome arrays were assembled on MSC or naked DNA substrates by an ATP-dependent system with native core histones and recombinant ACF in the presence of various combinations of chaperones: NAP-1, NLP, Nph, and TAP/p32. The assembly of nucleosome arrays was assayed as in *B*. (*Left* lane) The 123-bp DNA ladder.

and are involved in nucleosome assembly and remodeling. During metazoan evolution, however, their biochemical activities may have been harnessed for SCR owing to biochemical similarities (net charge and amino acid composition) and functional roles (DNA compaction) of histones and protamines.

Although yeast TAP/p32 ortholog Mam33p is clearly involved in regulation of DNA integrity/repair in response to treatment with mutagens (Supplemental Fig. S3B) and genetically interacts with factors of chromatin remodeling and DNA compaction and repair (Supplemental Fig. S3C), it is also required for metabolism of alternative carbon sources (Supplemental Fig. S3A). Similarly, mammalian TAP/p32 has also been implicated in mitochondrial function (Brokstad et al. 2001). Furthermore, *Drosophila* TAP/p32 and NAP-1, although subject to nuclear translocation, are also efficiently recruited to mitochondria (Supplemental Fig. S2C). Hence, it is interesting to consider the apparent dual role of TAP/p32 in mitochondrial function and nuclear DNA compaction. Mature sperm cells in *Drosophila* and vertebrates contain a stack of mitochondrial structures in the midpiece at the junction of the head and tail. (In *Drosophila*, the sperm mitochondria are depleted of DNA [DeLuca and O'Farrell 2012], and, in most metazoan species during fertilization, sperm mitochondria undergo rapid ubiquitination and degradation by autophagocytosis [Sutovsky et al. 1999; Al Rawi et al. 2011].) Thus, the elevated affinity of TAP/p32 and NAP-1 to protein components of mitochondria may be used and adapted for rapid and specific recruitment of the TAP/p32 and NAP-1 to the sperm head, which would facilitate their loading onto sperm chromatin for its processing.

It has been suggested that *Xenopus* nucleoplasmin is sufficient for the initial stage of SCR (decondensation of demembranated sperm and removal of sperm basic proteins SP1–6 in vitro) (Philpott et al. 1991; Philpott and Leno 1992). However, the removal of sperm proteins (and their replacement by histones) in the presence of nucleoplasmin does not appear complete/quantitative (Philpott and Leno 1992; Katagiri and Ohsumi 1994). Furthermore, the *Xenopus* sperm decondensation assay is prone to artifacts: It is frequently performed (and works) with heterologous proteins and extracts, including those from yeast (Ito et al. 1996a; Harkness 2006). In contrast, our analyses suggest that a family of several factors may share

partially redundant roles in protamine removal, and their cooperative action is necessary and sufficient for complete protamine eviction from sperm chromatin substrates. On the other hand, considering poor evolutionary conservation of protamine number and identities, it is possible that species other than *Drosophila* use smaller or larger sets of factors for SCR.

Despite being ~94% identical (Supplemental Fig. S1A), protamines A and B require different chaperones for their removal. For instance, in the absence of TAP/p32, a mixture of NAP-1, NLP, and Nph is incapable of protamine B eviction (Fig. 3E–G). Protamine polypeptides are extremely evolutionarily divergent. In fact, it is rarely possible to assign a protamine function based on a sequence conservation search of related proteins in distinct metazoan species. For example, a closely related organism, *Drosophila simulans*, expresses one protein homologous to *D. melanogaster* protamines. It is more closely related to protamine B and shares with it only 77% identity. *D. simulans* also express orthologs of protamine chaperones. A high degree of functional/sequence specificity makes it unlikely that *D. melanogaster* protamine chaperones will be able to remodel MSC assembled from more divergent, evolutionarily distant protamines. This specificity may contribute to gametic isolation of distinct species (Markow 1997). In the future, it will be interesting to analyze cross-reactivity of protamines and protamine chaperones from these species in MSC remodeling in vitro and in vivo.

Materials and methods

Recombinant proteins, reconstitution, and analyses of MSC substrate

Full-length *Drosophila* protamines A and B (Mst35Ba and Mst35Bb proteins), untagged and C-terminally V5-tagged, were cloned as chimeras with C-terminal intein–chitin-binding domain tags in a modified pTXB1 vector. cDNA was prepared by PCR from expressed sequence tags SD20170 and GH11850. Full-length cDNA for NLP, Nph, and TAP/p32 (LD16456-, SD23244-, and LD29590-expressed sequences tags, respectively) were amplified by PCR and cloned in-frame with C-terminal 6-His tag into pET-29b vector (Novagen). Proteins were expressed in *Escherichia coli* (Rosetta strain, Invitrogen) and purified as described (Fyodorov and Kadonaga 2003). See the Supplemental Material for details.

MSC was reconstituted by salt dialysis as described for oligonucleosome arrays (Emelyanov et al. 2010). Restriction enzyme accessibility assay, topoisomerase I treatment, partial micrococcal nuclease and DNase I digestion, and in vitro ChIP were performed as described (Fyodorov and Kadonaga 2003; Emelyanov et al. 2010; Lu et al. 2013) using naked supercoiled DNA, salt-dialyzed chromatin, or MSC as a substrate. For detailed conditions, see the Supplemental Material.

ATP-dependent nucleosome assembly and protamine eviction reactions

Oligonucleosome assembly with S-190 extract and purified recombinant system was performed exactly as described (Fyodorov and Levenstein 2002; Fyodorov and Kadonaga 2003). For protamine eviction analyses, MSC substrate (equivalent to 20 μg of plasmid DNA) was treated with 4 mL of S-190 extract, fractionated by sucrose gradient sedimentation, and analyzed by anti-V5 Western blotting. Alternatively, protamines were evicted from MSC by incubating 0.47 pmol of substrate (~1 μg of DNA) with >20-fold molar excess of recombinant NAP-1, NLP, Nph, and TAP/p32, and the reactions were fractionated on gravity-flow size exclusion columns. See the Supplemental Material for reaction conditions and details of analyses.

For purification of putative protamine chaperones, sucrose gradient fractions that contained V5-immunoreactive material were pooled and immunoprecipitated with anti-V5-agarose (Sigma).

Antibodies and immunoblotting

Polyclonal antibodies to recombinant Nph and TAP/p32 were raised in guinea pigs (Pocono Rabbit Farm and Laboratory). Rabbit polyclonal antibody to NLP was a gift of Jim Kadonaga (University of California at San Diego). To examine expression of NLP and Nph in vivo, whole L3 larvae were ground, and the homogenates were subjected to Western analyses. Subcellular localization analyses were performed exactly as described (Kang et al. 1995). Details of fractionation and Western blotting are described in the Supplemental Material.

Analyses of chaperone–histone interactions by glycerol gradient sedimentation

Recombinant protamine chaperones (~100 μg) were incubated for 20 min on ice with 25 μg of native *Drosophila* core histones in buffer R plus 150 mM NaCl and fractionated on 20%–50% glycerol gradient in buffer R with protease inhibitors (see above) and 0.01% NP-40 in a Beckman SW-55 rotor at 50,000 rpm for 16 h. The gradients were cut into 10 fractions and analyzed by SDS-PAGE and Coomassie staining.

Fly genetics

Flies were grown on standard corn meal, sugar, and yeast medium with Tegosept. Stocks and crosses were maintained at 25°C except when otherwise indicated. Null *P32* alleles were prepared by a modified protocol for ends-out homologous recombination (Huang et al. 2008). *Df(3R)Nph[Nlp]* was generated by imprecise excision of *P{EPgy2}EY21985* P-element as described (Fyodorov et al. 2004). Other stocks were obtained from the Bloomington Stock Center.

For viability analyses, parents with single or double heterozygous or homozygous mutations were mated inter se or with appropriate counterparts as shown in Tables 1 and 2, and eclosion of homozygous mutant progeny was scored based on balancer markers. Fecundity and embryonic lethality in *P32* mutants were analyzed as described (Novoseltsev et al. 2005). See the Supplemental Material for details of genetic experiments.

Staining of Drosophila *embryos*

For embryonic stage analyses, wild-type or $P32^2/P32^4$ mutant embryos were collected 0–2 h and 0–4 h AED and stained with 5 μg/mL PI. Prior to PI staining, the embryos were incubated for 1 h in a solution containing 2 μg/mL RNase A at 55°C. VectaShield-mounted preparations were observed under a Zeiss Axiovert 200M. For each experiment, 500 embryos were scored.

Acknowledgments

We are grateful to J. Kadonaga and Y. Hong for antibodies, purified proteins, plasmids and fly lines. We thank K. Beirit,

A. Konev, A. Lusser, and D. Shechter for critical reading of the manuscript and valuable suggestions. We also thank V. Nikitina for help analyzing the SGA data. Protein sequencing was performed by the Proteomics Resource Center at Rockefeller University. This work was supported by grants from the National Institutes of Health to D.V.F. (GM074233) and M.C.K (ES019966), and an National Cancer Institute Cancer Center Support Grant to Albert Einstein College of Medicine (CA013330).

References

Akey CW, Luger K. 2003. Histone chaperones and nucleosome assembly. *Curr Opin Struct Biol* **13:** 6–14.

Al Rawi S, Louvet-Vallee S, Djeddi A, Sachse M, Culetto E, Hajjar C, Boyd L, Legouis R, Galy V. 2011. Postfertilization autophagy of sperm organelles prevents paternal mitochondrial DNA transmission. *Science* **334:** 1144–1147.

Ashburner M, Misra S, Roote J, Lewis SE, Blazej R, Davis T, Doyle C, Galle R, George R, Harris N, et al. 1999. An exploration of the sequence of a 2.9-Mb region of the genome of *Drosophila melanogaster*: the Adh region. *Genetics* **153:** 179–219.

Balasundaram D, Dinman JD, Tabor CW, Tabor H. 1994. SPE1 and SPE2: two essential genes in the biosynthesis of polyamines that modulate +1 ribosomal frameshifting in *Saccharomyces cerevisiae*. *J Bacteriol* **176:** 7126–7128.

Balhorn R. 1982. A model for the structure of chromatin in mammalian sperm. *J Cell Biol* **93:** 298–305.

Balhorn R. 2007. The protamine family of sperm nuclear proteins. *Genome Biol* **8:** 227.

Bellen HJ, Gregory BK, Olsson CL, Kiger JA Jr. 1987. Two *Drosophila* learning mutants, dunce and rutabaga, provide evidence of a maternal role for cAMP on embryogenesis. *Dev Biol* **121:** 432–444.

Beltrao P, Cagney G, Krogan NJ. 2010. Quantitative genetic interactions reveal biological modularity. *Cell* **141:** 739–745.

Berro R, Kehn K, de la Fuente C, Pumfery A, Adair R, Wade J, Colberg-Poley AM, Hiscott J, Kashanchi F. 2006. Acetylated Tat regulates human immunodeficiency virus type 1 splicing through its interaction with the splicing regulator p32. *J Virol* **80:** 3189–3204.

Bonnefoy E, Orsi GA, Couble P, Loppin B. 2007. The essential role of *Drosophila* HIRA for de novo assembly of paternal chromatin at fertilization. *PLoS Genet* **3:** 1991–2006.

Brokstad KA, Kalland KH, Russell WC, Matthews DA. 2001. Mitochondrial protein p32 can accumulate in the nucleus. *Biochem Biophys Res Commun* **281:** 1161–1169.

Bruni R, Roizman B. 1996. Open reading frame P—a herpes simplex virus gene repressed during productive infection encodes a protein that binds a splicing factor and reduces synthesis of viral proteins made from spliced mRNA. *Proc Natl Acad Sci* **93:** 10423–10427.

Burns KH, Viveiros MM, Ren Y, Wang P, DeMayo FJ, Frail DE, Eppig JJ, Matzuk MM. 2003. Roles of NPM2 in chromatin and nucleolar organization in oocytes and embryos. *Science* **300:** 633–636.

Crevel G, Cotterill S. 1995. DF 31, a sperm decondensation factor from *Drosophila melanogaster*: purification and characterization. *EMBO J* **14:** 1711–1717.

DeLuca SZ, O'Farrell PH. 2012. Barriers to male transmission of mitochondrial DNA in sperm development. *Dev Cell* **22:** 660–668.

Dilworth SM, Black SJ, Laskey RA. 1987. Two complexes that contain histones are required for nucleosome assembly in vitro: role of nucleoplasmin and N1 in *Xenopus* egg extracts. *Cell* **51:** 1009–1018.

Dutta S, Akey IV, Dingwall C, Hartman KL, Laue T, Nolte RT, Head JF, Akey CW. 2001. The crystal structure of nucleoplasmin-core: implications for histone binding and nucleosome assembly. *Mol Cell* **8:** 841–853.

Eisen JA, Sweder KS, Hanawalt PC. 1995. Evolution of the SNF2 family of proteins: subfamilies with distinct sequences and functions. *Nucleic Acids Res* **23:** 2715–2723.

Emelyanov AV, Konev AY, Vershilova E, Fyodorov DV. 2010. Protein complex of *Drosophila* ATRX/XNP and HP1a is required for the formation of pericentric β-heterochromatin in vivo. *J Biol Chem* **285:** 15027–15037.

Emelyanov AV, Vershilova E, Ignatyeva MA, Pokrovsky DK, Lu X, Konev AY, Fyodorov DV. 2012. Identification and characterization of ToRC, a novel ISWI-containing ATP-dependent chromatin assembly complex. *Genes Dev* **26:** 603–614.

Fyodorov DV, Kadonaga JT. 2003. Chromatin assembly in vitro with purified recombinant ACF and NAP-1. *Methods Enzymol* **371:** 499–515.

Fyodorov DV, Levenstein ME. 2002. Chromatin assembly in *Drosophila* systems. *Curr Protoc Mol Biol* **58:** 21.7.1–21.7.27.

Fyodorov DV, Blower MD, Karpen GH, Kadonaga JT. 2004. Acf1 confers unique activities to ACF/CHRAC and promotes the formation rather than disruption of chromatin in vivo. *Genes Dev* **18:** 170–183.

Ghebrehiwet B, Lim BL, Peerschke EI, Willis AC, Reid KB. 1994. Isolation, cDNA cloning, and overexpression of a 33-kD cell surface glycoprotein that binds to the globular 'heads' of C1q. *J Exp Med* **179:** 1809–1821.

Gorbalenya AW, Koonin EV. 1993. Helicases: amino acid sequence comparisons and structure-function relationships. *Curr Opin Struct Biol* **3:** 419–429.

Guruharsha KG, Rual JF, Zhai B, Mintseris J, Vaidya P, Vaidya N, Beekman C, Wong C, Rhee DY, Cenaj O, et al. 2011. A protein complex network of *Drosophila melanogaster*. *Cell* **147:** 690–703.

Hamasaki-Katagiri N, Tabor CW, Tabor H. 1997. Spermidine biosynthesis in *Saccharomyces cerevisae*: polyamine requirement of a null mutant of the SPE3 gene (spermidine synthase). *Gene* **187:** 35–43.

Hammoud SS, Nix DA, Zhang H, Purwar J, Carrell DT, Cairns BR. 2009. Distinctive chromatin in human sperm packages genes for embryo development. *Nature* **460:** 473–478.

Harkness TA. 2006. Decondensation of *Xenopus* sperm chromatin using *Saccharomyces cerevisiae* whole-cell extracts. *Can J Physiol Pharmacol* **84:** 451–458.

Haushalter KA, Kadonaga JT. 2003. Chromatin assembly by DNA-translocating motors. *Nat Rev Mol Cell Biol* **4:** 613–620.

Hoppins S, Collins SR, Cassidy-Stone A, Hummel E, Devay RM, Lackner LL, Westermann B, Schuldiner M, Weissman JS, Nunnari J. 2011. A mitochondrial-focused genetic interaction map reveals a scaffold-like complex required for inner membrane organization in mitochondria. *J Cell Biol* **195:** 323–340.

Huang J, Zhou W, Watson AM, Jan YN, Hong Y. 2008. Efficient ends-out gene targeting in *Drosophila*. *Genetics* **180:** 703–707.

Ito T, Bulger M, Kobayashi R, Kadonaga JT. 1996a. *Drosophila* NAP-1 is a core histone chaperone that functions in ATP-facilitated assembly of regularly spaced nucleosomal arrays. *Mol Cell Biol* **16:** 3112–3124.

Ito T, Tyler JK, Bulger M, Kobayashi R, Kadonaga JT. 1996b. ATP-facilitated chromatin assembly with a nucleoplasmin-like protein from *Drosophila melanogaster*. *J Biol Chem* **271:** 25041–25048.

Ito T, Bulger M, Pazin MJ, Kobayashi R, Kadonaga JT. 1997. ACF, an ISWI-containing and ATP-utilizing chromatin assembly and remodeling factor. *Cell* **90:** 145–155.

Ito T, Levenstein ME, Fyodorov DV, Kutach AK, Kobayashi R, Kadonaga JT. 1999. ACF consists of two subunits, Acf1 and ISWI, that function cooperatively in the ATP-dependent catalysis of chromatin assembly. *Genes Dev* **13:** 1529–1539.

Jayaramaiah Raja S, Renkawitz-Pohl R. 2005. Replacement by *Drosophila melanogaster* protamines and Mst77F of histones during chromatin condensation in late spermatids and role of sesame in the removal of these proteins from the male pronucleus. *Mol Cell Biol* **25:** 6165–6177.

Jiang J, Zhang Y, Krainer AR, Xu RM. 1999. Crystal structure of human p32, a doughnut-shaped acidic mitochondrial matrix protein. *Proc Natl Acad Sci* **96:** 3572–3577.

Kang D, Nishida J, Iyama A, Nakabeppu Y, Furuichi M, Fujiwara T, Sekiguchi M, Takeshige K. 1995. Intracellular localization of 8-oxo-dGTPase in human cells, with special reference to the role of the enzyme in mitochondria. *J Biol Chem* **270:** 14659–14665.

Katagiri C, Ohsumi K. 1994. Remodeling of sperm chromatin induced in egg extracts of amphibians. *Int J Dev Biol* **38:** 209–216.

Kawasaki K, Philpott A, Avilion AA, Berrios M, Fisher PA. 1994. Chromatin decondensation in *Drosophila* embryo extracts. *J Biol Chem* **269:** 10169–10176.

Konev AY, Tribus M, Park SY, Podhraski V, Lim CY, Emelyanov AV, Vershilova E, Pirrotta V, Kadonaga JT, Lusser A, et al. 2007. CHD1 motor protein is required for deposition of histone variant H3.3 into chromatin in vivo. *Science* **317:** 1087–1090.

Krainer AR, Conway GC, Kozak D. 1990. Purification and characterization of pre-mRNA splicing factor SF2 from HeLa cells. *Genes Dev* **4:** 1158–1171.

LeRoy G, Orphanides G, Lane WS, Reinberg D. 1998. Requirement of RSF and FACT for transcription of chromatin templates in vitro. *Science* **282:** 1900–1904.

LeRoy G, Loyola A, Lane WS, Reinberg D. 2000. Purification and characterization of a human factor that assembles and remodels chromatin. *J Biol Chem* **275:** 14787–14790.

Lewis PW, Elsaesser SJ, Noh KM, Stadler SC, Allis CD. 2010. Daxx is an H3.3-specific histone chaperone and cooperates with ATRX in replication-independent chromatin assembly at telomeres. *Proc Natl Acad Sci* **107:** 14075–14080.

Loppin B, Berger F, Couble P. 2001. The *Drosophila* maternal gene *sésame* is required for sperm chromatin remodeling at fertilization. *Chromosoma* **110:** 430–440.

Loppin B, Bonnefoy E, Anselme C, Laurencon A, Karr TL, Couble P. 2005. The histone H3.3 chaperone HIRA is essential for chromatin assembly in the male pronucleus. *Nature* **437:** 1386–1390.

Lu X, Wontakal SN, Kavi H, Kim BJ, Guzzardo PM, Emelyanov AV, Xu N, Hannon GJ, Zavadil J, Fyodorov DV, et al. 2013. *Drosophila* H1 regulates the genetic activity of heterochromatin by recruitment of Su(var)3-9. *Science* **340:** 78–81.

Luger K, Mader AW, Richmond RK, Sargent DF, Richmond TJ. 1997. Crystal structure of the nucleosome core particle at 2.8 Å resolution. *Nature* **389:** 251–260.

Lusser A, Urwin DL, Kadonaga JT. 2005. Distinct activities of CHD1 and ACF in ATP-dependent chromatin assembly. *Nat Struct Mol Biol* **12:** 160–166.

Lutas A, Wahlmark CJ, Acharjee S, Kawasaki F. 2012. Genetic analysis in *Drosophila* reveals a role for the mitochondrial protein p32 in synaptic transmission. *G3 (Bethesda)* **2:** 59–69.

Mack PD, Kapelnikov A, Heifetz Y, Bender M. 2006. Mating-responsive genes in reproductive tissues of female *Drosophila melanogaster*. *Proc Natl Acad Sci* **103:** 10358–10363.

Markow TA. 1997. Assortative fertilization in *Drosophila*. *Proc Natl Acad Sci* **94:** 7756–7760.

Matsumoto K, Nagata K, Miyaji-Yamaguchi M, Kikuchi A, Tsujimoto M. 1999. Sperm chromatin decondensation by template activating factor I through direct interaction with basic proteins. *Mol Cell Biol* **19:** 6940–6952.

Matthews DA, Russell WC. 1998. Adenovirus core protein V interacts with p32—a protein which is associated with both the mitochondria and the nucleus. *J Gen Virol* **79:** 1677–1685.

McLay DW, Clarke HJ. 2003. Remodelling the paternal chromatin at fertilization in mammals. *Reproduction* **125:** 625–633.

Mello JA, Almouzni G. 2001. The ins and outs of nucleosome assembly. *Curr Opin Genet Dev* **11:** 136–141.

Messerschmitt M, Jakobs S, Vogel F, Fritz S, Dimmer KS, Neupert W, Westermann B. 2003. The inner membrane protein Mdm33 controls mitochondrial morphology in yeast. *J Cell Biol* **160:** 553–564.

Miller D, Brinkworth M, Iles D. 2010. Paternal DNA packaging in spermatozoa: more than the sum of its parts? DNA, histones, protamines and epigenetics. *Reproduction* **139:** 287–301.

Muta T, Kang D, Kitajima S, Fujiwara T, Hamasaki N. 1997. p32 protein, a splicing factor 2-associated protein, is localized in mitochondrial matrix and is functionally important in maintaining oxidative phosphorylation. *J Biol Chem* **272:** 24363–24370.

Namboodiri VM, Dutta S, Akey IV, Head JF, Akey CW. 2003. The crystal structure of *Drosophila* NLP-core provides insight into pentamer formation and histone binding. *Structure* **11:** 175–186.

Novoseltsev VN, Arking R, Carey JR, Novoseltseva JA, Yashin AI. 2005. Individual fecundity and senescence in *Drosophila* and medfly. *J Gerontol A Biol Sci Med Sci* **60:** 953–962.

Okuwaki M, Sumi A, Hisaoka M, Saotome-Nakamura A, Akashi S, Nishimura Y, Nagata K. 2012. Function of homo- and hetero-oligomers of human nucleoplasmin/nucleophosmin family proteins NPM1, NPM2 and NPM3 during sperm chromatin remodeling. *Nucleic Acids Res* **40:** 4861–4878.

Orsi GA, Algazeery A, Meyer RE, Capri M, Sapey-Triomphe LM, Horard B, Gruffat H, Couble P, Ait-Ahmed O, Loppin B. 2013. *Drosophila* Yemanuclein and HIRA cooperate for de novo assembly of H3.3-containing nucleosomes in the male pronucleus. *PLoS Genet* **9:** e1003285.

Pazin MJ, Kamakaka RT, Kadonaga JT. 1994. ATP-dependent nucleosome reconfiguration and transcriptional activation from preassembled chromatin templates. *Science* **266:** 2007–2011.

Petersen-Mahrt SK, Estmer C, Ohrmalm C, Matthews DA, Russell WC, Akusjarvi G. 1999. The splicing factor-associated protein, p32, regulates RNA splicing by inhibiting ASF/SF2 RNA binding and phosphorylation. *EMBO J* **18:** 1014–1024.

Philpott A, Leno GH. 1992. Nucleoplasmin remodels sperm chromatin in *Xenopus* egg extracts. *Cell* **69:** 759–767.

Philpott A, Leno GH, Laskey RA. 1991. Sperm decondensation in *Xenopus* egg cytoplasm is mediated by nucleoplasmin. *Cell* **65:** 569–578.

Piatti P, Zeilner A, Lusser A. 2011. ATP-dependent chromatin remodeling factors and their roles in affecting nucleosome fiber composition. *Int J Mol Sci* **12:** 6544–6565.

Rathke C, Baarends WM, Awe S, Renkawitz-Pohl R. 2014. Chromatin dynamics during spermiogenesis. *Biochim Biophys Acta* **1839:** 155–168.

Ray-Gallet D, Quivy JP, Scamps C, Martini EM, Lipinski M, Almouzni G. 2002. HIRA is critical for a nucleosome assembly pathway independent of DNA synthesis. *Mol Cell* **9:** 1091–1100.

Reinders J, Zahedi RP, Pfanner N, Meisinger C, Sickmann A. 2006. Toward the complete yeast mitochondrial proteome: multidimensional separation techniques for mitochondrial proteomics. *J Proteome Res* **5:** 1543–1554.

Schnakenberg SL, Matias WR, Siegal ML. 2011. Sperm-storage defects and live birth in *Drosophila* females lacking spermathecal secretory cells. *PLoS Biol* **9:** e1001192.

Stephens GE, Xiao H, Lankenau DH, Wu C, Elgin SC. 2006. Heterochromatin protein 2 interacts with Nap-1 and NURF: a link between heterochromatin-induced gene silencing and the chromatin remodeling machinery in *Drosophila*. *Biochemistry* **45:** 14990–14999.

Sutovsky P, Moreno RD, Ramalho-Santos J, Dominko T, Simerly C, Schatten G. 1999. Ubiquitin tag for sperm mitochondria. *Nature* **402:** 371–372.

Tagami H, Ray-Gallet D, Almouzni G, Nakatani Y. 2004. Histone H3.1 and H3.3 complexes mediate nucleosome assembly pathways dependent or independent of DNA synthesis. *Cell* **116:** 51–61.

Tange TO, Jensen TH, Kjems J. 1996. In vitro interaction between human immunodeficiency virus type 1 Rev protein and splicing factor ASF/SF2-associated protein, p32. *J Biol Chem* **271:** 10066–10072.

Torigoe SE, Patel A, Khuong MT, Bowman GD, Kadonaga JT. 2013. ATP-dependent chromatin assembly is functionally distinct from chromatin remodeling. *eLife* **2:** e00863.

Van Holde RE. 1988. *Chromatin*. Springer Verlag, New York.

Varga-Weisz PD, Wilm M, Bonte E, Dumas K, Mann M, Becker PB. 1997. Chromatin-remodelling factor CHRAC contains the ATPases ISWI and topoisomerase II. *Nature* **388:** 598–602.

Wang Y, Finan JE, Middeldorp JM, Hayward SD. 1997. P32/TAP, a cellular protein that interacts with EBNA-1 of Epstein-Barr virus. *Virology* **236:** 18–29.

Ward WS, Coffey DS. 1991. DNA packaging and organization in mammalian spermatozoa: comparison with somatic cells. *Biol Reprod* **44:** 569–574.

Wolffe AP. 1998. *Chromatin: structure and function*. Academic Press, New York.

Wright SJ, Longo FJ. 1988. Sperm nuclear enlargement in fertilized hamster eggs is related to meiotic maturation of the maternal chromatin. *J Exp Zool* **247:** 155–165.

Yu L, Zhang Z, Loewenstein PM, Desai K, Tang Q, Mao D, Symington JS, Green M. 1995. Molecular cloning and characterization of a cellular protein that interacts with the human immunodeficiency virus type 1 Tat transactivator and encodes a strong transcriptional activation domain. *J Virol* **69:** 3007–3016.